

PRODUCTION OF LIKE SIGN DI-LEPTONS IN $p - p$
COLLISIONS THROUGH COMPOSITE MAJORANA
NEUTRINOS.

O. Panella^{*(a)}, C. Carimalo^(b) and Y. N. Srivastava^(a,c)

^{a)}*Istituto Nazionale di Fisica Nucleare, Sezione di Perugia,
Via A. Pascoli, I-06123 Perugia, Italy*

^{b)}*Laboratoire de Physique Nucléaire et de Hautes Energies, IN2P3-CNRS
Universités Paris VI/VII,
4 place Jussieu, F-75252, Paris Cedex 05, France*

^{c)}*Northeastern University, Physics Department, Boston Ma, 02115*

DRAFT # 4

(February 1, 2020)

*Author to whom correspondence should be addressed.

Electronic address: Orlando.Panella@PG.infn.it

Abstract

The production of Like-Sign-Di-leptons (LSD), in the high energy lepton number violating ($\Delta L = +2$) reaction, $pp \rightarrow 2\text{jets} + \ell^+\ell^+$, ($\ell = e, \mu, \tau$), of interest for the experiments to be performed at the forthcoming Large Hadron Collider (LHC), is investigated in detail, taking up a composite model scenario in which the exchanged virtual *composite* neutrino is assumed to be a Majorana particle that couples to the light leptons via the $SU(2) \times U(1)$ gauge bosons through a magnetic type coupling ($\sigma_{\mu\nu}$). An helicity projection method is used to evaluate exactly the tree-level amplitudes of the contributing parton subprocesses ($2 \rightarrow 4$), which allows to take into account all exchange diagrams and occurring interferences. Numerical estimates of the corresponding signal cross-section that implement kinematical cuts needed to suppress the Standard Model background, are presented which show that in some regions of the parameter space the total number of LSD events is well above the background. Assuming non-observation of the LSD signal it is found that LHC would exclude a composite Majorana neutrino up to 850 GeV (if one requires 10 events for discovery). The sensitivity of LHC experiments to the parameter space is then compared to that of the next generation of neutrinoless double beta decay ($\beta\beta_{0\nu}$) experiment, GENIUS, and it is shown that they will provide constraints of the same order of magnitude and will play a complementary role.

12.60.Rc, 14.60.St, 13.15.+g, 13.85.Rm, 23.40.-s

I. INTRODUCTION

Since the discovery of the Z^0 and W^\pm gauge bosons [1] the standard model (SM) of electroweak interactions [2] based on the $SU(2)\times U(1)$ gauge group has scored an impressive record of experimental checks. However some unexplained facts of the model like the mass hierarchy, the proliferation of elementary particles, and the total number of free parameters have lead to believe that it is only a low energy manifestation of a yet unknown underlying fundamental theory, which would be free of the above theoretical difficulties. Therefore despite the enormous experimental success of the SM many alternative theories have been developed such as Left-Right symmetric models, composite models, super-symmetry, string theory, grand unified models. The investigation of effects predicted by the new theories that are absent in the standard theory is therefore very important since, were these effects to be experimentally observed they would signal *new physics* unaccounted for by the SM. It is in this direction that a great portion of recent theoretical and experimental studies have been concentrated [4], and this is indeed the spirit of this work which deals with lepton number violating processes.

The conservation of the total lepton number (L) is one of the symmetries of the SM experimentally observed to hold true until now. In the SM with massless Dirac neutrinos processes with $\Delta L \neq 0$ are not possible. Violation of this symmetry is generally related to the existence of massive Majorana particles and many extensions of the SM contain L -violating interactions involving Majorana neutrinos. Left-Right symmetric models for example contain right-handed Majorana neutrinos, with a mass that could be in the TeV range, and coupled to the light leptons via the right-handed gauge bosons (W_R, Z_R) [5]. Superstring generated E_6 models also have neutral Majorana leptons [6]. Finally ref. [7] provides an example of a composite model with Majorana neutrals.

The effect which seems most promising with respect to showing violations of the lepton number is the neutrinoless double beta decay ($\beta\beta_{0\nu}$), a second order process where, in a nucleus, two protons (neutrons) undergo simultaneously a weak beta decay emitting two

positrons (electrons) while the two neutrinos annihilate into the vacuum [4]:

$$A(Z + 2) \rightarrow A(Z) + e^+e^+ \quad \Delta L = +2 \quad (1)$$

This process is only possible if the neutrino is a massive Majorana particle, and thus it is impossible within the SM. Experiments that search for such rare decay have since long been performed but always with negative results [3]. Currently the Heidelberg-Moscow $\beta\beta$ experiment at the Gran-Sasso laboratory in Italy provides the best experimental lower bound on the half-life of the process [8]:

$$\begin{aligned} & {}^{76}\text{Ge} \rightarrow {}^{76}\text{Se} + 2e^- \\ & T_{1/2}^{\beta\beta_{0\nu}} > 1.2 \times 10^{25} \text{yr.} \end{aligned} \quad (2)$$

The proposed GENIUS double beta experiment (see section VI), now under development, will either increase the lower bound on the half-life by two or three orders of magnitude or observe the decay. From the theoretical point of view, the strong bound on the half-life in Eq. (2) has been turned into a powerful tool to impose constraints on models of new physics which predict a non zero amplitude for the $\beta\beta_{0\nu}$ decay [9]. Studies in this direction include: an investigation of new super-symmetric contributions from R-parity violating MSSM [10] which shows how constraints on parameters of the model from non-observation of $\beta\beta_{0\nu}$ are stronger than those available from accelerator experiments; a detailed analysis of the contribution to $\beta\beta_{0\nu}$ from left-right symmetric models [11]; a study of the effective low energy charged current lepton-quark interactions due to the exchange of heavy leptoquarks [12].

The present authors have, in a series of recent papers [13–15], investigated the contribution, to the neutrinoless double beta decay, of a heavy Majorana neutrino, arising from a composite model scenario in which the excited partner of the neutrino (the excited neutrino, ν^*) is assumed to be a Majorana particle. This study revealed that $\beta\beta_{0\nu}$ constraints are competitive, and in some regions of the parameter space, even more restrictive than those derived from high-energy direct search of excited particles [15,16]. This result led to consider the potential of the experiments to be performed at the forthcoming Large Hadron Collider

(LHC) at CERN, with respect to the possibility of observing the production of Like Sign Di-leptons, $\ell^+\ell^+$ or $\ell^-\ell^-$, $\ell = e, \mu, \tau$, (hereafter denoted LSD) in proton-proton collisions with an energy of 14 TeV in the center of mass frame:

$$pp \rightarrow 2\text{jets} + \text{LSD}, \quad \Delta L = +2. \quad (3)$$

In hadronic collisions LSD can be produced in quark-quark (antiquark-antiquark) scattering, through the elementary sub-process $W^+W^+ \rightarrow \ell^+\ell^+$ (virtual W -boson fusion) as depicted in Fig. 1 where the dashed blob represents all contributing diagrams within a given model. As regards this mechanism of LSD production one can say that it is the high-energy analog of the neutrinoless double beta decay which indeed proceeds through the same Feynman diagrams (see for example ref. [15]). Fig. 2a shows explicitly the Feynman diagram for the production of LSD through the exchange of a heavy Majorana neutrino, (basic mechanism). In the case of quark-antiquark scattering in addition to the W fusion another mechanism must be considered that leads to LSD production: the direct production of a heavy Majorana neutrino via quark-antiquark annihilation, $q\bar{q}' \rightarrow \ell^+N$, with the subsequent decay of the heavy neutrino $N \rightarrow \ell^+q\bar{q}'$ (annihilation mechanism). This is depicted in Fig. 2b.

Production of LSD has been considered in the past by several authors and within the context of different models. In the Left-Right symmetric model, Keung and Senjanović [17] already in 1983 realized that the associate production of LSD with two hadronic jets would signal the annihilation of quark-antiquark pairs into the right-handed gauge boson of the model (W_R). Estimates were given for pp collisions at $\sqrt{s} = 800$ GeV. The study of this model was later taken up to higher energies (SSC and LHC) by Datta, Guchait and Roy in [18] where the authors indicated how to effectively reduce the SM background. Dicus, Karatas and Roy [19] have studied LSD production at high-energy hadron colliders through the exchange of heavy right-handed Majorana neutrinos, without commitment to a specific model (beyond the SM). They used a γ_μ -type coupling and found the LSD signal detectable at the SSC while at the LHC the SM background would probably preclude detection. Two of the present authors [20] provided a rough estimate of the signal cross

sections for $pp \rightarrow 2\text{jets} + \text{LSD}$ at LHC within the context of composite models (exchange of a heavy composite Majorana neutrino with a $\sigma_{\mu\nu}$ -type coupling) using an equivalent W-boson approximation [21] (similar to the Weiszäcker Williams approximation for the photon field) and integrating over the complete phase-space of the sub-process $W^+W^+ \rightarrow \ell^+\ell^+$. The result was that the signal could be observable at the LHC.

One remark should be made at this point that applies to all works just cited that have investigated LSD production in pp collisions. None of them deals, *at the same time*, with the two mechanisms of LSD production, i.e. W^+W^+ -fusion and $q\bar{q}'$ -annihilation. Indeed when dealing with $q\bar{q}'$ scattering both mechanisms must be considered and the corresponding amplitudes should be added coherently. In order to do so one needs a way of efficiently computing the amplitudes. In this paper it is done precisely so, calculating analytically the helicity amplitudes of the occurring tree-level diagrams and accounting thus for the interference term between the W^+W^+ -fusion and the $q\bar{q}'$ -annihilation.

Thus the goal of this paper is twofold: (i) to address the sensitivity of LHC experiments with respect to the parameters of the composite model effective Lagrangian and compare this to that of the next generation of double beta decay experiments now under development (GENIUS); (ii) to present a calculation of LSD production in pp collisions (via the exchange of a heavy composite Majorana neutrino) which goes beyond the approximations of [20] and which, in the case of $q\bar{q}'$ -annihilation, includes coherently the two competing mechanisms.

The rest of the paper is organised as follows: in section II the reader is briefly reminded of the effective Lagrangian describing the coupling of the excited neutrino with the electron and a comparison between recent bounds on the parameters from the low energy $\beta\beta_{0\nu}$ experiment by the Heidelberg-Moscow Collaboration and those from high energy experiments performed by the DELPHI Collaboration at the Large Electron Positron (LEP) Collider is presented; in section III the amplitudes of the L-violating parton sub-processes are presented; section IV contains: (i) a description of the kinematical cuts applied with a short discussion of the background; (ii) our numerical results for the signal cross-sections; in section V the sensitivity to the parameter space of LHC is compared to that of GENIUS; finally, section

VI contains the conclusions.

II. COMPOSITENESS AND EXISTING $\beta\beta_{0\nu}$ CONSTRAINTS.

It is well known that one possible scenario of physics beyond the SM is one in which quarks and leptons are not elementary particles but possess an internal structure, i.e. they are bound states of, yet unknown, new constituents, generally referred to as *preons*, bound together by a new dynamical interaction. Theories that follow this path are called *composite models* and although many have been proposed [22] none has emerged as a new dynamically consistent theory. However there are some model independent consequences of the idea of compositeness which can be addressed without commitment to any specific model. These are: (i) contact interactions between ordinary fermions; (ii) the existence of excited partners for quarks and leptons with masses of the order of the compositeness scale, Λ_C . Phenomenologically these ideas have been studied via effective interactions [14,23]. In particular in this work, the case of excited neutrinos (N), is taken up and only the relevant coupling with the light electron are reviewed. Effective couplings between the heavy and light leptons (or quarks) have been proposed, using weak iso-spin (I_W) and hyper-charge (Y) conservation [24]. Assuming that such states are grouped in $SU(2) \times U(1)$ multiplets, since light fermions have $I_W = 0, 1/2$ and electroweak gauge bosons have $I_W = 0, 1$, only multiplets with $I_W \leq 3/2$ can be excited in the lowest order perturbation theory. Also, since none of the gauge fields carry hyper-charge, a given excited multiplet can couple only to a light multiplet with the same Y . The transition coupling of heavy-to-light fermions is assumed to be of the magnetic moment type respect to any electroweak gauge bosons [24]. Restrict here to the first family and consider spin-1/2 excited states grouped in multiplets with $I_W = 1/2$ and $Y = -1$ (the so called homodoublet model [23]),

$$L = \begin{pmatrix} N \\ E \end{pmatrix} \quad (4)$$

which can couple to the light left-handed multiplet

$$\ell_L = \begin{pmatrix} \nu_L \\ e_L \end{pmatrix} = \frac{1 - \gamma_5}{2} \begin{pmatrix} \nu \\ e \end{pmatrix} \quad (5)$$

through the gauge fields \vec{W}^μ and B^μ . The relevant interaction is written [24] in terms of two *new* independent coupling constants f and f' :

$$\begin{aligned} \mathcal{L}_{int} = & \frac{gf}{\Lambda_C} \bar{L} \sigma_{\mu\nu} \frac{\vec{\tau}}{2} l_L \cdot \partial^\nu \vec{W}^\mu \\ & + \frac{g'f'}{\Lambda_C} \left(-\frac{1}{2} \bar{L} \sigma_{\mu\nu} l_L \right) \cdot \partial^\nu B^\mu + \text{h.c.} \end{aligned} \quad (6)$$

where $\vec{\tau}$ are the Pauli $SU(2)$ matrices, g and g' are the usual $SU(2)$ and $U(1)$ gauge coupling constants, and the factor of $-1/2$ in the second term is the hyper-charge of the $U(1)$ current. This effective Lagrangian is widely used in the literature to predict production cross sections and decay rates of the excited particles [23,25,26]. In terms of the physical gauge fields the interaction Lagrangian describing the coupling of the heavy excited neutrino with the light electron is therefore:

$$\mathcal{L}_{eff} = \left(\frac{gf}{\sqrt{2}\Lambda_C} \right) \left\{ \left(\bar{N} \sigma^{\mu\nu} \frac{1 - \gamma_5}{2} e \right) \partial_\nu W_\mu^+ \right\} + \text{H.c.} \quad (7)$$

In the analysis carried out in [13,14] it was assumed that the excited neutrino is a Majorana particle with mass M_N , expected to be of the order of the compositeness scale Λ_C , which would then contribute to the neutrinoless double beta decay. The following result for the half-life of the $\beta\beta_{0\nu}$ was found [14]:

$$T_{1/2}^{-1} = \left(\frac{f}{\Lambda_C} \right)^4 \frac{m_A^8}{M_N^2} |\mathcal{M}_{FI}|^2 \frac{G_{01}}{m_e^2}, \quad (8)$$

where $m_A = 0.85$ GeV is a parameter entering the nuclear form factors, $\mathcal{M}_{FI} = -5.45 \times 10^{-2}$ is a nuclear matrix element, m_e is the electron mass and $G_{01} = 6.4 \times 10^{-15}$ yr $^{-1}$ is a phase space integral. Combining this result with the non-observation of the decay ($T_{1/2} > T_{1/2}^{\text{lower bound}}$) one obtains a constraint on the parameters of the model:

$$\left| \frac{f}{\Lambda_C} \right| < M_N^{1/2} \left(\frac{m_e^2}{m_A^8} \right)^{1/4} \frac{[G_{01} T_{1/2}^{\text{lower bound}}]^{-1/4}}{|\mathcal{M}_{FI}|^{1/2}}. \quad (9)$$

Using the current experimental lower bound on the half-life of the ^{76}Ge decay provided by the Heidelberg-Moscow $\beta\beta$ experiment, the following constraint on the parameters $f, \Lambda_{\text{C}}, M_N$ appearing in Eq. (7) is deduced ¹:

$$|f| \leq 8.03 \frac{\Lambda_{\text{C}}}{1 \text{ TeV}} \left(\frac{M_N}{1 \text{ TeV}} \right)^{1/2}. \quad (10)$$

This double beta bound on compositeness can be compared with bounds on the same parameters from high energy experiments performed at the Large Electron Positron (LEP) collider, phase II. The DELPHI Collaboration has reported [27] on a search for excited leptons in e^+e^- collisions at $\sqrt{s} = 183 \text{ GeV}$, where both the single and double production mode were studied. It should be emphasized that the analysis in [27] was carried out using the same effective Lagrangian that was considered in [13,14], c.f. Eq.(7), so that it makes sense to compare the corresponding bounds. In Fig. 3 the bound of Eq. 10 is plotted against the exclusion curve of the DELPHI Collaboration [27], and one can see that for masses above $\approx 110 \text{ GeV}$ the double beta bound is more constraining, i.e. it excludes a portion of parameter phase space still allowed by the DELPHI exclusion plot². This result prompted the present authors to study the potential of the LHC with respect to the same type of lepton number violating processes, with an emphasis on comparing its sensitivity with that of the next generation of double beta decay experiments. The following section deals with

¹This is an updated constraint respect to that of ref. [13] where a previous value of the half-life was used.

²It should be noted that also the ALEPH Collaboration has recently published results of a search for compositeness at LEP I. In ref. [28] bounds on the compositeness scale, in particular regarding the same excited neutrino couplings discussed here, are reported. Choosing $f = f' = 1$ a neutrino mass dependent lower bound on Λ_{C} is found which is about 16 TeV at $M_N = \mathcal{O}(10 \text{ GeV})$ while it drops down to 4 TeV at the maximum value of M_N explored of 80 GeV. This result is not directly comparable to Eq. (10) since this was derived within the hypothesis $M_N \gg M_W$ [15]. Assuming $|f| = 1$, Eq. (10) gives : $\Lambda_{\text{C}} \geq 0.12 \text{ TeV}$ at $M_N = 1 \text{ TeV}$.

the calculation of the lepton number violating processes in pp collisions described by the diagrams of Figures 1 and 2. They have been carried out with a choice of the parameters that satisfies the bounds from $\beta\beta_{0\nu}$ just discussed.

III. AMPLITUDES OF L -VIOLATING PARTON SUB-PROCESSES

In the following the helicity amplitudes for parton sub-processes that contribute to production of LSD via the exchange (or production) of a heavy Majorana composite neutrino are presented. The effective interaction used is that of Eq. (7). Considering for the moment only the first family, three different types of processes should be distinguished:

$$\begin{aligned}
(i) \quad & uu \rightarrow dd + \ell^+ \ell^+, \\
(ii) \quad & u\bar{d} \rightarrow d\bar{u} + \ell^+ \ell^+, \\
(iii) \quad & \bar{d}\bar{d} \rightarrow \bar{u}\bar{u} + \ell^+ \ell^+.
\end{aligned} \tag{11}$$

The amplitudes are written using the following definitions of propagator factors:

$$\begin{aligned}
1/A &= [(p_a - p_c)^2 - M_W^2] [(p_b - p_d)^2 - M_W^2] \\
1/B &= [(p_a - p_d)^2 - M_W^2] [(p_b - p_c)^2 - M_W^2] \\
1/\tilde{A} &= [(p_a + p_b)^2 - M_W^2 + iM_W\Gamma_W] [(p_c + p_d)^2 - M_W^2 + iM_W\Gamma_W]
\end{aligned} \tag{12}$$

$$\begin{aligned}
C &= (p_a - p_c - p_e)^2 - M_N^2 \\
D &= (p_a - p_c - p_f)^2 - M_N^2 \\
E &= (p_a - p_d - p_e)^2 - M_N^2 \\
F &= (p_a - p_d - p_f)^2 - M_N^2 \\
\tilde{C} &= (p_c + p_d + p_e)^2 - M_N^2 + iM_N\Gamma_N \\
\tilde{D} &= (p_c + p_d + p_f)^2 - M_N^2 + iM_N\Gamma_N
\end{aligned} \tag{13}$$

The width of the heavy composite neutrino, Γ_N , is of course a quantity which depends on the free parameters of the particular model that is being considered here, $|f|, \Lambda_C$ and

M_N , and has been the object of discussion in the literature [35,26]. Typically the width of excited leptons (quarks) receives contributions from the gauge interactions of Eq. (7) and from contact terms arising from novel *strong* preon interactions [26]³. In order to keep the numerical computations of cross-sections presented in the following reasonably simple, a constant value of $\Gamma_N = 70$ GeV has been adopted, which is a somewhat average value in the mass range considered.

Define also the quantities:

$$\begin{aligned} s(m, n) &= s(p_m, p_n) = \bar{u}_+(p_m)u_-(p_n), \\ t(m, n) &= t(p_m, p_n) = \bar{u}_-(p_m)u_+(p_n), \end{aligned} \tag{14}$$

which are given by:

$$\begin{aligned} s(m, n) &= -2\sqrt{E_m E_n} G_{mn}, \\ t(m, n) &= +2\sqrt{E_m E_n} F_{mn}, \end{aligned} \tag{15}$$

with

$$\begin{aligned} G_{mn} &= \cos(\theta_m/2) \sin(\theta_n/2) e^{+i(\phi_m - \phi_n)/2} - \sin(\theta_m/2) \cos(\theta_n/2) e^{-i(\phi_m - \phi_n)/2}, \\ F_{mn} &= (G_{mn})^*. \end{aligned} \tag{16}$$

Let the tensor $T_{\mu\nu}$ describe the virtual sub-process $W^*W^* \rightarrow \ell^+\ell^+$ (Fig. 2a), while the tensor $\tilde{T}_{\mu\nu}$ describes the virtual sub-process $(W^*)^+ \rightarrow \ell^+\ell^+(W^*)^-$ appearing in the diagram of Fig. 2b. $J_{a,c}$ and $\bar{J}_{b,d}$, are the quark (antiquark) currents that couple in the t-channel to the virtual gauge bosons of the standard model (Fig. 2a) while $\tilde{J}_{a,b}$ and $\tilde{J}_{c,d}^*$, are the incoming and outgoing currents of the $q\bar{q}'$ pair that couples in the s-channel to the W-bosons (Fig. 2b).

³It is to be noted however that these contact terms while contributing to the total width of the excited neutrino cannot contribute to the production of LSD via the diagrams discussed in this work.

$$\begin{aligned}
J_{a,c}^\mu &= \bar{u}(p_c) \gamma^\mu \frac{1-\gamma_5}{2} u(p_a) \\
\bar{J}_{b,d}^\mu &= \bar{v}(p_b) \gamma^\mu \frac{1-\gamma_5}{2} v(p_d) \\
\tilde{J}_{a,b}^\mu &= \bar{v}(p_b) \gamma^\mu \frac{1-\gamma_5}{2} u(p_a) \\
(\tilde{J}_{c,d}^\mu)^* &= \bar{u}(p_c) \gamma^\mu \frac{1-\gamma_5}{2} v(p_d) .
\end{aligned} \tag{17}$$

the amplitudes are (unitary gauge):

$$(i) \quad \underline{U_i U_j \rightarrow D_k D_l + \ell^+ \ell^+}$$

$$\mathcal{M} = \mathcal{K} \bar{u}(p_e) \left\{ V_{U_i D_k} V_{U_j D_l} A \left[J_{(a,c)}^\mu T_{\mu\nu} J_{(b,d)}^\nu \right] - V_{U_i D_l} V_{U_j D_k} B \left[(p_c \leftrightarrow p_d) \right] \right\} v(p_f); \tag{18}$$

$$(ii) \quad \underline{U_i \bar{D}_j \rightarrow D_k \bar{U}_l + \ell^+ \ell^+}$$

$$\begin{aligned}
\mathcal{M}(WW - \text{fusion}) &= \mathcal{K} V_{U_i D_k} (V_{U_l D_j})^* \bar{u}(p_e) \left[A J_{(a,c)}^\mu T_{\mu\nu} \bar{J}_{(b,d)}^\nu \right] v(p_f); \\
\mathcal{M}(q\bar{q}' - \text{annihilation}) &= \mathcal{K} V_{U_i D_j} (V_{U_l D_k})^* \bar{u}(p_e) \left[\tilde{A} \tilde{J}_{(a,b)}^\mu \tilde{T}_{\mu\nu} (\tilde{J}_{(c,d)}^\nu)^* \right] v(p_f);
\end{aligned} \tag{19}$$

$$(iii) \quad \underline{\bar{D}_i \bar{D}_j \rightarrow \bar{U}_k \bar{U}_l + \ell^+ \ell^+}$$

$$\mathcal{M} = \mathcal{K} \bar{u}(p_e) \left\{ V_{U_k D_i}^* V_{U_l D_j}^* A \left[\bar{J}_{(a,c)}^\mu T_{\mu\nu} \bar{J}_{(b,d)}^\nu \right] - V_{U_l D_i}^* V_{U_k D_j}^* B \left[(p_c \leftrightarrow p_d) \right] \right\} v(p_f); \tag{20}$$

where U_i denotes a positively charged quark (up-type) while D_i denotes a negatively charged one (down-type). The quantities $V_{U_i D_j}$ are the elements of the CKM mixing matrix. Of course the annihilation diagram of Fig. 2a comes in only in quark-antiquark scattering. In processes (i) and (iii) the part of the amplitude depending on the factor B is due to the diagrams obtained exchanging the final state quarks. In the framework of the effective Lagrangian c.f. Eq. (7), as discussed in section II, it is found:

$$\begin{aligned}
T_{\mu\nu} &= \left[\frac{\sigma_{\mu\rho} \sigma_{\nu\sigma}}{C} + \frac{\sigma_{\nu\sigma} \sigma_{\mu\rho}}{D} \right] \frac{1-\gamma_5}{2} (p_a - p_c)^\rho (p_c - p_d)^\sigma, \\
\tilde{T}_{\mu\nu} &= \left[\frac{\sigma_{\mu\rho} \sigma_{\nu\sigma}}{\tilde{C}} + \frac{\sigma_{\nu\sigma} \sigma_{\mu\rho}}{\tilde{D}} \right] \frac{1-\gamma_5}{2} (p_a + p_b)^\rho (p_c + p_d)^\sigma, \\
\mathcal{K} &= \frac{g^4}{4} \left(\frac{f}{\Lambda_C} \right)^2 M_N.
\end{aligned} \tag{21}$$

Due to the chiral nature of the couplings involved, the calculation is particularly simple if performed in the helicity basis [29]. In the massless approximation only one helicity amplitude is non zero. The following result is found:

(i) $\underline{U_i U_j \rightarrow D_k D_l + \ell^+ \ell^+}$

$$\mathcal{M} = 4\mathcal{K} s(a, b) \left\{ \begin{aligned} & V_{U_i D_k} V_{U_j D_l} A t(a, c) t(d, b) \left[\frac{s(e, a) s(b, f)}{C} - \frac{s(f, a) s(b, e)}{D} \right] \\ & - V_{U_i D_l} V_{U_j D_k} B t(a, d) t(c, b) \left[\frac{s(e, a) s(b, f)}{E} - \frac{s(f, a) s(b, e)}{F} \right] \end{aligned} \right\}, \quad (22)$$

(ii) $\underline{U_i \bar{D}_j \rightarrow D_k \bar{U}_l + \ell^+ \ell^+}$

- (WW – fusion) :

$$\mathcal{M} = +4\mathcal{K} V_{U_i D_k} (V_{U_l D_j})^* A s(a, d) t(a, c) t(d, b) \left\{ \left[\frac{s(e, a) s(d, f)}{C} - \frac{s(f, a) s(d, e)}{D} \right] \right\}, \quad (23)$$

- ($q\bar{q}'$ – annihilation) :

$$\mathcal{M} = -4\mathcal{K} V_{U_i D_j} (V_{U_l D_k})^* \tilde{A} t(a, b) s(a, d) t(d, c) \left\{ \left[\frac{s(e, a) s(d, f)}{\tilde{C}} - \frac{s(f, a) s(d, e)}{\tilde{D}} \right] \right\}, \quad (24)$$

(iii) $\underline{\bar{D}_i \bar{D}_j \rightarrow \bar{U}_k \bar{U}_l + \ell^+ \ell^+}$

$$\mathcal{M} = 4\mathcal{K} s(c, d) \left\{ \begin{aligned} & (V_{U_k D_i})^* (V_{U_l D_j})^* A t(a, c) t(d, b) \left[\frac{s(e, c) s(d, f)}{C} - \frac{s(f, c) s(d, e)}{D} \right] \\ & + (V_{U_l D_i})^* (V_{U_k D_j})^* B t(a, d) t(c, b) \left[\frac{s(e, d) s(c, f)}{E} - \frac{s(f, d) s(c, e)}{F} \right] \end{aligned} \right\}. \quad (25)$$

The above simple analytic form of the amplitudes is also very easy to implement in a code for numerical applications, since the quantities $s(p_i, p_j)$ and $u(p_i, p_j)$ are just functions of the energies and angles of the particle's momenta, c.f. Equations (15) and (16).

IV. DISCUSSION AND RESULTS.

Before giving details of numerical calculations of the signal cross-section and discussing the results one should remind that there are processes of the standard model that also lead to LSD production and are thus sources of background to the signal. This question was already considered in refs [18,19]. An immediate source of background comes from the subprocesses $uu \rightarrow ddW^+W^+$, $u\bar{d} \rightarrow d\bar{u}W^+W^+$, $\bar{d}\bar{d} \rightarrow \bar{u}\bar{u}W^+W^+$ and similar ones involving higher-generation quarks and antiquarks, each W subsequently decaying into $\ell\nu_\ell$.

The corresponding overall reaction $pp \rightarrow 2\text{jets } \ell\nu_\ell \ell\nu_\ell$ can mimic the signal when the total missing P_T carried away by the neutrinos is small. As shown in [19], that background can be most efficiently reduced to a percent of fb in LHC conditions, which will be shown to be at the same level of the signal, in some regions of the parameter space, or even well below the latter in other regions. This background reduction is accomplished by limiting the missing P_T of neutrinos, that is, requiring a “ P_T -conservation” which is actually a characteristic of the signal.

As also observed in [18,19], a copious and more dangerous source of standard-model background seems to be due to $t\bar{t}$ production from gluon and quark initial states. In that process, one has the decay chains $t \rightarrow bW^+$, $W^+ \rightarrow \ell\nu_\ell$ on one side, and $\bar{t} \rightarrow \bar{b}W^-$, $\bar{b} \rightarrow \bar{c}\ell\nu_\ell$, $W^- \rightarrow qq'$ on the other side. For LHC conditions, that reaction leads to a total production of about 4×10^6 LSD per year. Here again, a limitation of missing P_T together with the condition of large P_T leptons allow one to reduce substantially that background. The additional requirement of lepton isolation further reduces the background. But while the two requirements of missing P_T limitation and lepton isolation will certainly eliminate two other similar backgrounds coming from direct $c\bar{c}$ and $b\bar{b}$ production, that of $t\bar{t}$ production seems to remain, according to [18,19], at a level which might jeopardize measurement of the signal at LHC.

At this point, it is worth noticing that within the standard model one can observe in pp collisions not only events with like-sign di-leptons of a given species ($e^\pm e^\pm$, $\mu^\pm \mu^\pm$, $\tau^\pm \tau^\pm$), but also events with “hybrid” like-sign di-leptons (HLSL) such as $e^\pm \mu^\pm$, $e^\pm \tau^\pm$, $\mu^\pm \tau^\pm$, with practically the same production rate for all these events since the W 's decay into any $\ell\nu_\ell$ final state at the same rate. Thus, one can get an idea on the amount of standard-model LSD background and eventually make appropriate subtraction by comparing, under given kinematical constraints, LSD production with HLSL production. At LHC, it would be most probably a comparison between $\mu^\pm \mu^\pm$, $\tau^\pm \tau^\pm$ production and $\mu^\pm \tau^\pm$ production. Said differently, once appropriate kinematical cuts performed, any significant difference between LSD production and HLSL production would signal lepton number violating processes like

those here considered. However, let us remark that a no-deviation result could not rule out new physics models allowing for lepton mixing.

In any case let us remark that an analysis of the background dedicated specifically to the LHC experimental conditions, and perhaps more complete than that presented in [18,19], is necessary (including in particular a detailed calculation of the amplitude of the processes involved), and will be the matter of a forthcoming work. Here the estimate of the background given in [19] is assumed:

$$\sigma_{background} = 3 \times 10^{-2} \text{ fb.} \quad (26)$$

In order to compare the signal cross-section with Eq.(26) kinematical cuts as discussed in [19] are used. The following selection criteria are needed in order to ensure lepton and jet identification:

$$\begin{aligned} |\eta_{lep}| < 4 & \quad p_T(lep) > 5 \text{ GeV}, \\ |\eta_{jet}| < 4 & \quad p_T(jet) > 20 \text{ GeV}. \end{aligned} \quad (27)$$

The signal cross-sections are obtained by folding the square of the amplitudes with the four-particle phase-space and the parton distribution functions:

$$d\sigma = \int dx_a dx_b \frac{1}{1 + \delta_{ij}} \left[f_i(x_a, Q^2) f_j(x_b, Q^2) + x_a \leftrightarrow x_b \right] \times \frac{1}{2\hat{s}} |\mathcal{M}|^2 (2\pi)^4 \delta^4(p_a + p_b - \sum_{m=1}^4 p_m) \frac{1}{2} \left(1 - \frac{\delta_{kl}}{2}\right) \prod_{n=1}^4 \frac{d^3\mathbf{p}_n}{(2\pi)^3 2E_n}, \quad (28)$$

where $\hat{s} = x_a x_b S$ is the squared center of mass energy of the parton collision and the factor $(1/2)(1 - \delta_{kl}/2)$ accounts for the presence of the two identical fermions ($\ell^+ \ell^+$) and the possibly identical quarks U_k, U_l (\bar{U}_k, \bar{U}_l) in the final state. The distribution functions are those of Set 1.1 of Duke-Owens (updated version of Set 1) as described in [30] with $\Lambda_{QCD} = 177 \text{ MeV}/c$. $\sqrt{S} = 14 \text{ TeV}$ has been used while the scale Q^2 is fixed at the value $Q^2 = \hat{s}$. With a proper choice of the transverse axis the phase-space reduces to a nine-dimensional integration that is performed with the well known VEGAS [31] routine which is based on a Monte-Carlo algorithm. This allows easy implementation of kinematical cuts

as described above. As regards the $u\bar{d}$ process the interference between the WW-fusion and annihilation mechanisms is naturally taken into account since the two (complex) amplitudes are summed before squaring.

In Figs.(4 & 6) the integrated cross-section with the parameter $|f| = 1$, i.e. $\sigma_1 = \sigma(|f| = 1)$ is given. As $\mathcal{M} \propto f^2$, the total cross section for other values of $|f|$ can be easily recovered ($\sigma = |f|^4 \times \sigma_1$). Keeping fixed $|f| = 1$ there are other two parameters on which our signal rate is dependent: Λ_C and M_N . In order to sample different regions of the parameter space two cases have been considered. Case (a) $\Lambda_C = 1$ TeV, and case (b) $\Lambda_C = M_N$.

Case (a) is shown in Fig.(4) where cross-sections corresponding to the three subprocesses of the first quark family, c.f. Eq.(11), are plotted versus the mass of the excited Majorana neutrino M_N (Fig. 4a,4b,4c). Since the subprocess $\bar{d}\bar{d} \rightarrow \bar{u}\bar{u} + \ell^+\ell^+$ is weighted by sea-quark distribution functions it is totally negligible relative to the other two. In Fig.(4d) the *total cross section* is plotted versus M_N including contributions from other subprocesses with second generation quarks, (c, s) as described in the appendix. Some of these subprocesses are however weighted by off-diagonal elements of the CKM mixing matrix and therefore give only small corrections. The shape of the curves as a function of M_N is clearly understood since the only dependence on the new parameters is of the type ⁴:

$$\sigma \sim \left(\frac{|f|}{\Lambda_C}\right)^4 M_N^2 \int \sum_K \frac{1}{(K^2 - M_N^2)^2 + \theta(K^2)(M_N\Gamma_N)^2} \quad (29)$$

where K are different momenta flowing in the Majorana propagator. Thus in case (a), $\sigma \rightarrow 0$ as $M_N \rightarrow 0$ while $\sigma \sim M_N^{-2}$ as $M_N \rightarrow \infty$, and there is an intermediate region with a maximum. There is a mass interval from $M_N = 250$ GeV up to $M_N \approx 3$ TeV where σ_1

⁴It should be remarked that this is only true within the approximation of a constant width Γ_N for the heavy neutrino. Taking into account the dependence of Γ_N with the new physics parameters $|f|, M_N$ and Λ_C (and those pertaining to contact terms) could modify, to some extent, the contribution of the quark-antiquark scattering. However, as pointed out in ref. [26], Γ_N receives the largest contribution from contact terms which are independent of $|f|$.

is bigger than the lowest measurable cross-section of 10^{-2} fb that corresponds to one event per year given the luminosity $\mathcal{L}_0 = 100 \text{ fb}^{-1}$ (integrated over one year) planned at LHC. For example the total signal cross-section σ_1 is at most about 5×10^{-2} fb, which is at the same level (though bigger) of the background (Eq. 26), and would only give five events per year. It seems therefore that, *with this particular choice of parameters* [case (a) $\Lambda_C = 1 \text{ TeV}$, $|f| = 1$], the lepton number violating signal due to the composite Majorana neutrino would hardly be measurable, unless a better set of kinematical cuts is found that enhances the absolute value of the signal rate while reducing still further the background. However one should keep in mind the dependence on the parameter $|f|$, which in Fig.(4) has been fixed to $|f| = 1$. Since the signal cross section is proportional to $|f|^4$ even a slightly larger value of $|f|$ could increase sensibly the signal cross-section.

Case (b) is shown in Fig.(6) with the same notation as in Fig.(4). Again the subprocess $\bar{d}\bar{d} \rightarrow \bar{u}\bar{u} + \ell^+\ell^+$ [Fig.(6c)] is totally negligible relative to the other two. The different shape of the cross section σ_1 as a function of M_N is of course due to the choice $\Lambda_C = M_N$, which according to Eq.(29) gives roughly $\sigma_1 \sim M_N^{-6}$ as $M_N \rightarrow \infty$ while $\sigma_1 \sim M_N^{-2}$ as $M_N \rightarrow 0$. Thus σ_1 is strongly enhanced respect to case (a) for values of $M_N < 1 \text{ TeV}$, while for $M_N > 1 \text{ TeV}$ it will be severely decreased. The cross-section σ_1 will be measurable in the mass interval $M_N = 250 \text{ GeV}$ (400 events/year) up to $M_N \approx 1.4 \text{ TeV}$ (1 event/year). This portion of the parameter space has therefore the potential of giving rise to a signal with a substantially higher number of events respect to the background, at least up to $M_N = 850 \text{ GeV}$ (10 events/year).

Finally it should be remarked that the discussion so far has been quite general with respect to the lepton flavour and applicable to all three of them but, (LSD = $\ell^\pm\ell^\pm$, $\ell = e, \mu, \tau$) at the LHC, muons will be the leptons most easily detected while the other lepton flavours will be detectable but with lower efficiencies [33]. For this reason the numerical results presented here refer to only one lepton generation.

V. COMPARING THE LHC VS THE GENIUS POTENTIAL

This section contains a comparative discussion of the constraints on the parameters $|f|, M_N, \Lambda_C$ that could be derived by the non observation of the L -violating signals discussed in the previous section at the *high-energy* LHC experiments as opposed to those deriving from the non-observation of *low-energy* neutrinoless double beta decay experiments, present (Heidelberg-Moscow) and next-generation (GENIUS). The new $\beta\beta_{0\nu}$ GENIUS experiment, (GERmanium-detectors in liquid NITrogen as shielding in an UndergrounD Setup) [32], has the potential to improve by orders of magnitude the lower bound on the $\beta\beta_{0\nu}$ decay half-life. Monte-Carlo simulations have shown that in one (four) year(s) of measurement the lower bound will be increased respectively to [32,34]:

$$T_{1/2}^{0\nu} > 5.8 \times 10^{27} \text{ yr}, \quad [\text{one year}]$$

$$T_{1/2}^{0\nu} > 2.3 \times 10^{28} \text{ yr}. \quad [\text{four years}]$$

Figures 7 & 8 show the upper bound on the parameter $|f|$ as function of the heavy neutrino mass M_N for the two cases (a) and (b) defined in the previous section. The curves concerning the $\beta\beta_{0\nu}$ bound are based on formulas that can be found in [16] which relative to Eq. (10) above include small correction terms of order $\mathcal{O}(M_W/M_N)$. The LHC curves are found using the numerical cross-sections presented in the previous section, requiring 10 events/year as a criterion for discovery of the L -violating signal, and assuming an integrated luminosity of $\mathcal{L}_0 = 100 \text{ fb}^{-1}$ as before. Thus non-observation of the signal at LHC means that $|f|^4 \sigma_1(M_N, \Lambda_C) \mathcal{L}_0 < 10$, which is translated into a constraint on $|f|$ that is the corresponding LHC upper bound to that in Eq. (10) from $\beta\beta_{0\nu}$:

$$|f| < \left(\frac{10}{\sigma_1 \mathcal{L}_0} \right)^{1/4}. \quad (30)$$

From Figures 7 & 8 one can infer *lower bounds* on the composite neutrino mass (or equivalently the compositeness scale) by *assuming* the dimensionless coupling $|f| \sim \mathcal{O}(1)$. For case (a), Fig. 7, one obtains the bounds shown in Table I while in Table II the corresponding

bounds for case (b), Fig. 8, are given. One comment is in order here. The LHC curve in Fig. 7 has a different behaviour for $M_N < 1$ TeV as compared to those of the $\beta\beta_{0\nu}$. This is due to the fact that as $M_N \rightarrow 0$, $\sigma_1 \rightarrow 0$ and thus the LHC upper bound on $|f|$ becomes weaker and weaker. This does not happen in the $\beta\beta_{0\nu}$ whose squared amplitude behaves as $|\mathcal{M}_{\beta\beta_{0\nu}}|^2 \sim M_N^{-2}$ [15] and at lower masses gives a bigger effect and therefore a stronger constraint. It is for this reason that Table I, for case (a), does not show a lower bound on M_N for LHC. In case (b) if $|f| \sim \mathcal{O}(1)$ GENIUS-(1 yr) can exclude Majorana composite neutrinos up to a mass of $M_N \sim 700$ GeV, while LHC and GENIUS-(4 yr) can go up to about 850 GeV. It is important to realize that the *non-accelerator, low-energy*, GENIUS-4yr experiment has the potential to probe the compositeness scale into the TeV region.

At this point the reader should be made aware that investigations of the same type of effective Lagrangians for compositeness within the context of LHC experiments have already been reported in the literature. In particular while the production of excited quarks at LHC has been investigated both via magnetic type gauge (G) interactions and contact terms (CT) [35], the production of excited *leptons* has however been considered *only through CT* and a mass sensitivity of up to about 4 – 5 TeV is found [35]. This work is therefore the first report concerning excited leptons at LHC within the context of magnetic type gauge interactions, and, while the discovery limit derived for contact terms [14,35] cannot be directly compared with the constraints derived in [13–15] from the non-observation of $\beta\beta_{0\nu}$ (that were based on gauge interactions G), the discovery limit for LHC reported here (M_N up to 850 GeV) can be directly compared with that of $\beta\beta_{0\nu}$ as done explicitly in Table II and Figures 7 and 8.

Finally it is worthwhile to note the complementary role that accelerator (LHC) and non-accelerator experiments (GENIUS) can have. Figures 7 and 8 show explicitly that, in both cases (a) and (b), while for low masses the $\beta\beta_{0\nu}$ bound is more restrictive there is always a crossing point where the LHC constraint becomes stronger, though of the same order of magnitude.

VI. CONCLUSIONS

In this work the production of Like Sign Di-leptons (LSD) via the exchange of a heavy composite Majorana neutrino in pp collisions has been studied in detail at LHC energies. The coupling of the Majorana neutrino is assumed to be a gauge interaction of the magnetic moment type ($\sigma_{\mu\nu}$). The helicity amplitudes have been presented and the resulting cross-sections within kinematical cuts, needed to suppress the SM background down to the fb level, are reported. Regions of the parameter space are pinned down where the signal is well above the estimated background ($\Lambda_C = M_N, |f| \sim 1, M_N < 850$ GeV). However a study of the background specifically dedicated to the LHC experimental conditions would certainly be of help towards a better understanding of the lepton number violating processes discussed here. The comparison of the LHC potential with respect to observing L -violating processes with that of the new generation of the *non-accelerator type* $\beta\beta_{0\nu}$ experiment, GENIUS, shows how the two approaches, *high- vs. low-energy*, do play a complementary role.

The approach developed here to discuss LSD production via composite Majorana neutrinos at LHC is being extended to other models of physics beyond the SM which provide L -violating interactions. The results of these analysis will be reported elsewhere.

One final remark is to be added concerning the interplay of *low- vs. high-energy* facilities with respect to the study of lepton number violation. The class of diagrams that give rise to $\Delta L = \pm 2$ processes discussed in this work could also trigger lepton number violating rare Kaon decays such as $K^+ \rightarrow \pi^- e^+ e^+$. At the Frascati Φ -factory, DAΦNE [36] (presently under commissioning), these decays could either be observed or, otherwise, the corresponding bounds on the branching ratios are susceptible to be strengthened. The current bound on the branching ratio for the ($\Delta L = -2$) K^+ decay is $Br(K^+ \rightarrow \pi^- e^+ e^+) < 1.0 \times 10^{-8}$ [23], while the sensitivity of the KLOE experiment [37] to be performed at DAΦNE could reach the level of 10^{-9} ; the KLOE experiment might thus provide insights on lepton number violating interactions beyond the standard model. Work along these lines is in progress.

ACKNOWLEDGMENTS

The authors would like to thank M. Espirito-Santo, of the DELPHI Collaboration, for providing the data histogram plotted in Figure 3.

O. P. would like to acknowledge useful discussions with the experimental colleagues of the Compact Muon Solenoid (CMS) Collaboration, L. Servoli, P. Cenci G. M. Bilei and A. Nappi.

C. C. acknowledges support by a grant from the Istituto Nazionale di Fisica Nucleare of Italy (INFN), that allowed his stay in Perugia, where this work was completed. He is also indebted to Z. Ajaltouni (ALEPH Collaboration), F. Fleuret and S. Jan (ATLAS Collaboration) for useful discussions.

This project is partially supported by the EEC-TMR Program, Contract N. CT98-0169.

APPENDIX A: LIST OF PARTON SUBPROCESSES

A list of all subprocesses leading to the production of LSD within the first two families of quarks is:

(i) quark scattering, $U_i U_j \rightarrow D_k D_l + \ell^+ \ell^+$,

$(k = l)$	$(k \neq l)$
$uu \rightarrow dd [ss] + \ell^+ \ell^+$	$uu \rightarrow ds + \ell^+ \ell^+$
$cc \rightarrow ss [dd] + \ell^+ \ell^+$	$cc \rightarrow ds + \ell^+ \ell^+$
$uc \rightarrow ss [dd] + \ell^+ \ell^+$	$uc \rightarrow ds + \ell^+ \ell^+$

(ii) quark antiquark scattering ($U_i \bar{D}_j \rightarrow D_k \bar{U}_l + \ell^+ \ell^+$):

$u\bar{d} \rightarrow d\bar{u} [d\bar{c}, s\bar{u}, s\bar{c}] + \ell^+ \ell^+$
$u\bar{s} \rightarrow d\bar{c} [d\bar{u}, s\bar{u}, s\bar{c}] + \ell^+ \ell^+$
$c\bar{s} \rightarrow s\bar{c} [s\bar{u}, d\bar{c}, d\bar{u}] + \ell^+ \ell^+$
$c\bar{d} \rightarrow s\bar{u} [s\bar{c}, d\bar{c}, d\bar{u}] + \ell^+ \ell^+$

(iii) anti-quark scattering ($\bar{D}_i \bar{D}_i \rightarrow \bar{U}_k \bar{U}_l + \ell^+ \ell^+$) :

$(k = l)$	$(k \neq l)$
$\bar{d}\bar{d} \rightarrow \bar{u}\bar{u} [\bar{c}\bar{c}] + \ell^+ \ell^+$	$\bar{d}\bar{d} \rightarrow \bar{u}\bar{c} + \ell^+ \ell^+$
$\bar{s}\bar{s} \rightarrow \bar{c}\bar{c} [\bar{u}\bar{u}] + \ell^+ \ell^+$	$\bar{s}\bar{s} \rightarrow \bar{u}\bar{c} + \ell^+ \ell^+$
$\bar{d}\bar{s} \rightarrow \bar{u}\bar{u} [\bar{c}\bar{c}] + \ell^+ \ell^+$	$\bar{d}\bar{s} \rightarrow \bar{c}\bar{u} + \ell^+ \ell^+$

Numerical results reported in Figures 4d and 6d contain contributions from some of the processes listed above. Processes initiated by two *sea* partons and not receiving contribution from the annihilation diagram have not been considered since Fig. 4c and 6c show that they are clearly negligible. As regards quark scattering only two cases have been considered; sub-processes initiated by uu and uc collisions, *i.e.* with at least one u -quark in the initial state:

- uu initiated sub-processes

- the processes $uu \rightarrow dd + \ell^+ \ell^+$, $uu \rightarrow ds + \ell^+ \ell^+$ and $uu \rightarrow ss + \ell^+ \ell^+$ are factorized as follows:

$$|\mathcal{M}_{uu\text{-initiated}}|^2 = \left[1 + 2 \left| \frac{V_{us}}{V_{ud}} \right|^2 + \left| \frac{V_{us}}{V_{ud}} \right|^4 \right] \times |\mathcal{M}_{uu \rightarrow dd + \ell^+ \ell^+}|^2, \quad (\text{A1})$$

the additional factor of 2, in the equation above, accounts for the fact that the process $uu \rightarrow ds + \ell^+ \ell^+$ does not contain identical quarks in the final state as opposed to the processes $uu \rightarrow dd + \ell^+ \ell^+$ and $uu \rightarrow ss + \ell^+ \ell^+$ and thus for it Eq. 28 applies with $k \neq l$.

Quark-antiquark scattering sub-processes have been divided into:

- $u\bar{d}$ collisions

- the processes $u\bar{d} \rightarrow [d\bar{u}, s\bar{u}, d\bar{c}] + \ell^+ \ell^+$ are factorized as:

$$|\mathcal{M}_{u\bar{d}\text{-initiated}}|^2 = \left[1 + \left| \frac{V_{us}}{V_{ud}} \right|^2 + \left| \frac{V_{dc}}{V_{ud}} \right|^2 \right] \times |\mathcal{M}_{u\bar{d} \rightarrow d\bar{u} + \ell^+ \ell^+}|^2; \quad (\text{A2})$$

- the process $u\bar{d} \rightarrow s\bar{c} + \ell^+\ell^+$, that will turn out to be numerically the most important, between those containing second family partons, does not factorize as above due to the fact that the WW -fusion and the annihilation diagram come in with different factors of the elements of the CKM matrix:

$$|\mathcal{M}_{u\bar{d} \rightarrow s\bar{c} + \ell^+\ell^+}|^2 = \left| \frac{V_{us}V_{dc}}{V_{ud}^2} \mathcal{M}_{u\bar{d} \rightarrow d\bar{u} + \ell^+\ell^+}^{(WW-fusion)} + \frac{V_{cs}}{V_{ud}} \mathcal{M}_{u\bar{d} \rightarrow d\bar{u} + \ell^+\ell^+}^{(u\bar{d}-annihil.)} \right|^2, \quad (\text{A3})$$

(see Eq. 23).

• $u\bar{s}$ collisions

- the processes $u\bar{s} \rightarrow [s\bar{u}, d\bar{u}, s\bar{c}] + \ell^+\ell^+$ can be factorized as :

$$|\mathcal{M}_{u\bar{s}-initiated}|^2 = \left(\frac{V_{us}}{V_{ud}} \right)^4 \left[1 + \left| \frac{V_{us}}{V_{ud}} \right|^2 + \left| \frac{V_{cs}}{V_{us}} \right|^2 \right] \times |\mathcal{M}_{u\bar{d} \rightarrow d\bar{u} + \ell^+\ell^+}|^2, \quad (\text{A4})$$

and using the fact the within the set of parton densities used here (set 1.1 of Owens [30]), $\bar{u}(x) = \bar{d}(x) = \bar{s}(x)$, the cross section for $u\bar{s}$ initiated collisions can be simply obtained from $\sigma_1(u\bar{d} \rightarrow d\bar{u} + \ell^+\ell^+)$ by multiplying it with the above CKM factor wich is $0.054 \approx 5\%$;

- the process $u\bar{s} \rightarrow d\bar{c} + \ell^+\ell^+$ does not factorize as in the above equation and must be considered separately (it is shown in Fig. 5):

$$\mathcal{M}_{u\bar{s} \rightarrow d\bar{c} + \ell^+\ell^+} = \left| \frac{V_{cs}}{V_{ud}} \mathcal{M}_{u\bar{d} \rightarrow d\bar{u} + \ell^+\ell^+}^{(WW-fusion)} + \frac{V_{us}V_{dc}}{(V_{ud})^2} \mathcal{M}_{u\bar{d} \rightarrow d\bar{u} + \ell^+\ell^+}^{(u\bar{d}-annihil.)} \right|^2; \quad (\text{A5})$$

• $c\bar{s}$ collisions

- the processes $c\bar{s} \rightarrow [s\bar{c}, s\bar{u}, d\bar{c}] + \ell^+\ell^+$ can be factorized as :

$$\begin{aligned} |\mathcal{M}_{c\bar{s}-initiated}|^2 &= \left(\frac{V_{cs}}{V_{ud}} \right)^4 \left[1 + \left| \frac{V_{us}}{V_{cs}} \right|^2 + \left| \frac{V_{cd}}{V_{cs}} \right|^2 \right] \times |\mathcal{M}_{u\bar{d} \rightarrow d\bar{u} + \ell^+\ell^+}|^2, \\ &= \left[1 + \left| \frac{V_{us}}{V_{cd}} \right|^2 + \left| \frac{V_{cs}}{V_{cd}} \right|^2 \right] \times |\mathcal{M}_{c\bar{s} \rightarrow d\bar{c} + \ell^+\ell^+}|^2, \end{aligned}$$

- finally the process $c\bar{s} \rightarrow d\bar{u} + \ell^+\ell^+$ has to be considered separately:

$$|\mathcal{M}_{c\bar{s} \rightarrow d\bar{u} + \ell^+\ell^+}|^2 = \left| \frac{V_{cd}V_{us}}{V_{ud}^2} \mathcal{M}_{u\bar{d} \rightarrow d\bar{u} + \ell^+\ell^+}^{(WW-fusion)} + \frac{V_{cs}}{V_{ud}} \mathcal{M}_{u\bar{d} \rightarrow d\bar{u} + \ell^+\ell^+}^{(u\bar{d}-annihil.)} \right|^2; \quad (\text{A6})$$

- $c\bar{d}$ collisions

- the processes $c\bar{d} \rightarrow [s\bar{c}, d\bar{u}, d\bar{c}] + \ell^+\ell^+$ can be factorized as :

$$\begin{aligned} |\mathcal{M}_{c\bar{d}\text{-initiated}}|^2 &= \left(\frac{V_{cd}}{V_{ud}}\right)^2 \left[1 + \left|\frac{V_{cd}}{V_{ud}}\right|^2 + \left|\frac{V_{cs}}{V_{ud}}\right|^2\right] \times |\mathcal{M}_{u\bar{d}\rightarrow d\bar{u}+\ell^+\ell^+}|^2, \\ &= \left[1 + \left|\frac{V_{cd}}{V_{cs}}\right|^2 + \left|\frac{V_{ud}}{V_{cs}}\right|^2\right] \times |\mathcal{M}_{c\bar{s}\rightarrow d\bar{c}+\ell^+\ell^+}|^2, \end{aligned}$$

- finally the process $c\bar{d} \rightarrow s\bar{u} + \ell^+\ell^+$ has to be considered separately:

$$|\mathcal{M}_{c\bar{d}\rightarrow s\bar{u}+\ell^+\ell^+}|^2 = \left|\frac{V_{cs}}{V_{ud}}\mathcal{M}_{u\bar{d}\rightarrow d\bar{u}+\ell^+\ell^+}^{(WW\text{-fusion})} + \frac{V_{cd}V_{us}}{V_{ud}^2}\mathcal{M}_{u\bar{d}\rightarrow d\bar{u}+\ell^+\ell^+}^{(u\bar{d}\text{-annihil.})}\right|^2; \quad (\text{A7})$$

Finally the amplitude of the process $uc \rightarrow ds + \ell^+\ell^+$ although weighted by only one u-quark distribution function contains a graph multiplied by diagonal elements of the CKM matrix ($\propto V_{ud}^2V_{cs}^2$) and turns out to yield a contribution comparable to that of the $q\bar{q}'$ subprocesses described above (see Fig. 5).

Eqs. (A1-A5) have been adopted to estimate the contribution of the subprocesses due to second family partons. Note that in numerical computations, the complex phases of the elements of the CKM mixing matrix have been neglected, assuming $V_{ij} = |V_{ij}|$, as only the first two generations are being considered here.

APPENDIX B: SQUARE OF AMPLITUDES

For the convenience of the reader interested in numerical applications the square of the amplitudes of the WW fusion mechanism is given here expressed in terms of the particles' momenta scalar products. In the numerical calculations it has been checked that one obtains an agreement of 1 part in 10^5 between this way of calculating the square of the amplitudes and the other consisting in writing down complex amplitudes and numerically taking the square of the absolute value.

Defining the quantities $K_i (i = 1, 2, 3)$ by

$$\sum_{\text{pol}} |\mathcal{M}_i|^2 = 512 \mathcal{F}_{CKM}^{(i)} \mathcal{K}^2 K_i \quad (\text{B1})$$

they are explicitly:

$$(i) \underline{U_i U_j \rightarrow D_k D_l + \ell^+ \ell^+}$$

$$\begin{aligned}
K_i = p_a \cdot p_b \left\{ + A^2 p_a \cdot p_c p_b \cdot p_d \left[+ \frac{p_a \cdot p_e p_b \cdot p_f}{C^2} + \frac{p_a \cdot p_f p_b \cdot p_e}{D^2} - \frac{L(p_a, p_e, p_b, p_f)}{CD} \right] \right. \\
+ B^2 p_a \cdot p_d p_b \cdot p_c \left[+ \frac{p_a \cdot p_e p_b \cdot p_f}{E^2} + \frac{p_a \cdot p_f p_b \cdot p_e}{F^2} - \frac{L(p_a, p_e, p_b, p_f)}{EF} \right] \\
- AB \left\{ L(p_a, p_c, p_b, p_d) \left[\frac{p_a \cdot p_e p_b \cdot p_f}{CE} + \frac{p_a \cdot p_f p_b \cdot p_e}{DF} \right. \right. \\
\left. \left. - \frac{1}{2} L(p_a, p_e, p_b, p_f) \left(\frac{1}{CF} + \frac{1}{DE} \right) \right] \right. \\
\left. \left. - \frac{1}{2} \epsilon(p_a, p_b, p_c, p_d) \cdot \epsilon(p_a, p_b, p_e, p_f) \left(\frac{1}{CF} - \frac{1}{DE} \right) \right\} \right\} \quad (B2)
\end{aligned}$$

$$(ii) \underline{U_i \bar{D}_j \rightarrow D_k \bar{U}_l + \ell^+ \ell^+}$$

$$K_{ii} = p_a \cdot p_d p_b \cdot p_d p_c \cdot p_a A^2 \left\{ + \frac{p_e \cdot p_a p_f \cdot p_d}{C^2} + \frac{p_f \cdot p_a p_e \cdot p_d}{D^2} - \frac{L(p_e, p_a, p_f, p_d)}{CD} \right\} \quad (B3)$$

$$(iii) \underline{\bar{D}_i \bar{D}_j \rightarrow \bar{U}_k \bar{U}_l + \ell^+ \ell^+}$$

$$\begin{aligned}
K_{iii} = p_c \cdot p_d \left\{ + A^2 p_a \cdot p_c p_b \cdot p_d \left[+ \frac{p_c \cdot p_e p_f \cdot p_d}{C^2} + \frac{p_c \cdot p_f p_e \cdot p_d}{D^2} - \frac{L(p_c, p_e, p_d, p_f)}{CD} \right] \right. \\
+ B^2 p_a \cdot p_d p_b \cdot p_c \left[+ \frac{p_c \cdot p_f p_e \cdot p_d}{E^2} + \frac{p_c \cdot p_e p_f \cdot p_d}{F^2} - \frac{L(p_c, p_e, p_d, p_f)}{EF} \right] \\
- AB \left\{ L(p_a, p_c, p_b, p_d) \left[\frac{p_c \cdot p_e p_f \cdot p_d}{CF} + \frac{p_c \cdot p_f p_e \cdot p_d}{ED} \right. \right. \\
\left. \left. - \frac{1}{2} L(p_e, p_c, p_f, p_d) \left(\frac{1}{CE} + \frac{1}{DF} \right) \right] \right. \\
\left. \left. - \frac{1}{2} \epsilon(p_a, p_b, p_c, p_d) \cdot \epsilon(p_e, p_f, p_c, p_d) \left(\frac{1}{CE} - \frac{1}{DF} \right) \right\} \right\} \quad (B4)
\end{aligned}$$

with $L(p_a, p_b, p_c, p_d) = p_a \cdot p_b p_c \cdot p_d + p_a \cdot p_d p_b \cdot p_c - p_a \cdot p_c p_b \cdot p_d$.

REFERENCES

- [1] C. Rubbia, Rev. Mod. Phys. **57**, 699-722, (1985).
- [2] S. Weinberg, Phys. Rev. Lett. **19**, 1264 (1967).
A. Salam, in: *Elementary Particle Theory*, ed. N. Svartholm (Almqvist and Forlag, Stockholm, 1968).
- [3] For a review and further references see for example:
W. C. Haxton, G. J. Stephenson, Prog. Part. Nucl. Phys. **12**, 409-479, (1984).
- [4] Proceedings of the First International Conference on *Particle Physics Beyond the Standard Model*, Castle Ringberg, Germany, 8-14 June, 1997. “*Beyond the Desert 1997*”, Edited by H. V. Klapdor-Kleingrothaus and H. Päs, Institute of Physics Publishing, Bristol and Philadelphia, 1998.
- [5] J. C. Pati and A. Salam, Phys. Rev. D **10**, 275 (1974).
- [6] J. L. Hewett and T. G. Rizzo, Phys. Rep. **183**, 193 (1989).
- [7] R. Barbieri, R. N. Mohapatra and A. Masiero, Phys. Lett. **105B**, 369-374, (1981),
Erratum-ibid **107B**, 455-456, (1981).
- [8] H. V. Klapdor-Kleingrothaus, c.f. in [4], pag. 485.
- [9] Proceedings of the International Workshop “*Double Beta Decay and Related Topics*” held at the European Centre for Theoretical Studies (ECT*), Trento, Italy, April 24-May 5, 1995. Ed. H. V. Klapdor-Kleingrothaus and S. Stoica, World Scientific, Singapore, 1996.
- [10] M. Hirsch, H. V. Klapdor-Kleingrothaus and S. G. Kovalenko, Phys. Lett. B **352** (1995),
Phys. Rev. Lett. **75** (1995), 17; Phys. Rev. D **53** (1996) 1329.
- [11] M. Hirsch, H. V. Klapdor-Kleingrothaus and O. Panella, Phys. Lett. B **374**, 7-12, 1996;

- [12] M. Hirsch, H. V. Klapdor-Kleingrothaus and S. G. Kovalenko, Phys. Rev. D **54**, 4207-4210, 1996, Phys. Lett. B **378**, 17-22, 1996,
- [13] O. Panella and Y. N. Srivastava, Phys. Rev. D **52**, 5308-5313, 1995.
- [14] O. Panella in the proceedings of the Trento workshop c.f. [9].
- [15] O. Panella, C. Carimalo, Y. N. Srivastava and A. Widom, Phys. Rev. D **56**, 5766-5775, 1997.
- [16] O. Panella, C. Carimalo, Y. N. Srivastava and A. Widom, in “Beyond the Desert 1997”, c.f. [4].
- [17] Wai-Yee Keung and Goran Senjanović, Phys. Rev. Lett. **50**, 1427, (1983).
- [18] Amitava Datta, Manoranjan Guchait and D. P. Roy, Phys. Rev. D **47**, 961 (1993).
- [19] D. A. Dicus, D. D. Karatas and P. Roy Phys. Rev. D **44**, 2033 (1991).
- [20] O. Panella, *Ph. D. thesis*, 1991, Department of Physics, Northeastern University, Boston, Ma.
O. Panella, Y. N. Srivastava and A. Widom, Northeastern University Preprint 1991 (unpublished).
- [21] S. Dawson, Nucl. Phys. **B249**, 42-60, (1985).
- [22] H. Terazawa, Y. Chikashige and K. Akama, Phys Rev D **15** 480 (1977); H. Harari, Phys. Lett. B **86**, 83 (1979); H. Fritzsch, G. Mandelbaum, Phys. Lett. B **102**, 319 (1981); O. Greenberg and J. Schuler, *ibid* **99** 339 (1981); R. Barbieri, R. N. Mohapatra, A. Masiero, *ibid* 105 369 (1981).
For further references see for example: H. Harari, Phys. Rept. **104**, 159 (1984); I. A. D’Souza and C. S. Kalman, *Preons, Models of Leptons, Quarks and Gauge Bosons as Composite Objects*, World Scientific Publishing Co. Singapore, 1992.
- [23] R. M. Barnett *et al.* (Particle Data Group), *Review of Particle Properties*; Phys. Rev.

- D **54** 1, (1996).
- [24] N. Cabibbo, L. Maiani and Y. Srivastava, Phys. Lett. B **139** 459 (1984).
- [25] A. De Rujula, L. Maiani and R. Petronzio, Phys. Lett. B **140**, 253 (1984).
- [26] U. Baur, I. Hinchliffe and D. Zeppenfeld, Int. J. Mod. Phys. A **2** 1285, (1987).
- [27] DELPHI Collab.; Report No. CERN-EP/196, 1998.
- [28] R. Barate et al. (ALEPH Collab.); Eur. Phys. J. C **4**,571-590 (1998).
- [29] R. Kleiss and W. J. Stirling, Nucl. Phys. **B262** (1985) 235-262.
- [30] J. F. Owens, Phys. Lett. **B266** (1991), 126-130.
- [31] G. P. Lepage, J. Comput. Phys. **27**, 192, (1978).
- [32] J. Hellmig and H. V. Klapdor-Kleingrothaus, Preprint submitted to Zeit. Phys. C, 1997.
- [33] L. Servoli, (CMS Collaboration), private communication.
- [34] M. Hirsch, private communication.
- [35] A. Djouadi, J. Ng and T. G. Rizzo (unpublished); in: “*Electroweak Symmetry Breaking and Beyond the Standard Model*”, edited by T. Barklow, S. Dawson, H.E. Haber and S. Siegrist (World Scientific, Singapore, in press), hep-ph/9504210.
- U. Baur, M. Spira and P. M. Zerwas, Phys. Rev. D **42** 815-824 (1990).
- [36] The DAΦNE Project Team, “DAΦNE, Status and Plans”, Proceedings of PAC95 (1995).
- [37] The KLOE Collaboration, “Status of the KLOE experiment”, LNF-97/033 (1997).

TABLES

TABLE I. Lower bound on M_N for case (a) [$\Lambda_C = 1 \text{ TeV}$, $|f| = 1$]. The bounds are derived from the non observation of neutrinoless double beta decay ($\beta\beta_{0\nu}$) at the current (Heidelberg-Moscow) experiment and for the prospected GENIUS experiment after 1 and 4 years of running [32]. At LHC non observation of the LSD signal would not imply a lower bound on the composite neutrino mass because of the different shape of the exclusion plot. See Fig. 7.

Experiment	Exp. constraint	Lower Bound on M_N (GeV)
Heidelberg-Moscow	$T_{1/2} > 7.4 \times 10^{24} \text{ yr}$	$M_N > \sim 10$
GENIUS 1 yr	$T_{1/2} > 6.0 \times 10^{27} \text{ yr}$	$M_N > \sim 350$
GENIUS 4 yr	$T_{1/2} > 2.3 \times 10^{28} \text{ yr}$	$M_N > \sim 700$
LHC	$N_{events} < 10$	-----

TABLE II. Lower bound on M_N for case (b) [$\Lambda_C = M_N$, $|f| = 1$]. The bounds are derived from the non observation of neutrinoless double beta decay ($\beta\beta_{0\nu}$) at the current (Heidelberg-Moscow) experiment and for the prospected GENIUS experiment after 1 and 4 years of running [32] and from non observation of the LSD signal at LHC (less than 10 events in onen year). See Fig. 8.

Experiment	Exp. constraint	Lower Bound on M_N (GeV)
Heidelberg-Moscow	$T_{1/2} > 7.4 \times 10^{24} \text{ yr}$	$M_N > \sim 250$
GENIUS 1 yr	$T_{1/2} > 6.0 \times 10^{27} \text{ yr}$	$M_N > \sim 700$
GENIUS 4 yr	$T_{1/2} > 2.3 \times 10^{28} \text{ yr}$	$M_N > \sim 850$
LHC	$N_{events} < 10$	$M_N > \sim 850$

FIGURES

FIG. 1. Parton level mechanism for production of Like-Sign-Di-leptons (LSD) in high energy hadronic collisions. The shaded blob contains all contributing diagrams for the virtual subprocess $W^+W^+ \rightarrow \ell^+\ell^+$.

FIG. 2. Production of LSD through quark-antiquark scattering. There are here two interfering mechanisms to be considered : (a) virtual W fusion; (b) ℓ^+N_ℓ production via quark-antiquark annihilation with subsequent hadronic decay of the heavy neutrino $N_\ell \rightarrow \ell^+q\bar{q}$.

FIG. 3. Comparison between the $\beta\beta_{0\nu}$ and the LEP II upper bound on the quantity $|f|/(\sqrt{2}M_N)$ as a function of the heavy neutrino mass M_N , with the choice $\Lambda_C = M_N$. *Regions above the curves are excluded.*

FIG. 4. Cross section normalized to $|f| = 1$, *i.e.* $\sigma_1 = \sigma/|f|^4$ with the choice $\Lambda_C = 1$ TeV. (a) $uu \rightarrow dd + \ell^+\ell^+$; (b) $u\bar{d} \rightarrow d\bar{u} + \ell^+\ell^+$; (c) $\bar{d}\bar{d} \rightarrow \bar{u}\bar{u} + \ell^+\ell^+$, (d) the *solid* line is the sum of the contributions from Fig. 4a, 4b, 4c including factorizable corrections according to Eq. A1, A2; the *dashed* line is the process $u\bar{d} \rightarrow s\bar{c} + \ell^+\ell^+$ according to Eq. A3. Finally the *solid-diamond* line in (d) is the total cross section, σ_1 , including the sum of the sub-leading contributions reported in Fig. 5.

FIG. 5. Sub-leading processes: the *solid* line is the sum of $u\bar{s}$ collisions Eq. A4 and A5; the *long-dashed* line is the process $uc \rightarrow ds + \ell^+\ell^+$; the *dashed* is the sum of $c\bar{s}$ collisions, Eqs. A6 and A7; the dot-dashed line is the the sum of $c\bar{d}$ collisions, Eqs. A8 and A9. Finally the *solid-diamond* line is the total contribution to σ_1 of the above processes.

FIG. 6. Same as in Fig. 4 but with the choice $\Lambda_C = M_N$. As explained in the text the different shape of the cross-section σ_1 as function of M_N respect to Fig. 4 is because $\sigma_1 \propto \Lambda_C^{-4}$. Thus fixing $\Lambda_C = M_N$ gives of course a different function of M_N than choosing $\Lambda_C = 1$ TeV. The solid-diamond line in (d) again describes the total σ_1 as done in Fig. 4.

FIG. 7. Sensitivity of LHC vs. current and next generation (GENIUS) double beta experiments to the compositeness parameters. Case (a) $\Lambda_C = 1$ TeV. *Non-observation of the signal excludes regions above the curves.* If no signal will be observed both LHC and GENIUS will be able to get upper bounds on $|f|$ stronger by almost an order of magnitude respect to the present Heidelberg Moscow bound. There is a region where the LHC bound is weaker than the GENIUS 1 yr (4 yr) bound $M_N < 550$ (1000) GeV while for $M_N > 550$ (1000) GeV the LHC bound is stronger.

FIG. 8. Same as in Fig 7 but with $\Lambda_C = M_N$. Also here *regions above the curves are excluded.* Here the shape of the LHC exclusion plot is similar to that of $\beta\beta_{0\nu}$. The values of M_N at which the LHC curve crosses those of GENIUS are the same as in Fig. 7.

Fig. 1
 O. Panella, C. Carimalo and Y. N. Srivastava
 Physical Review D

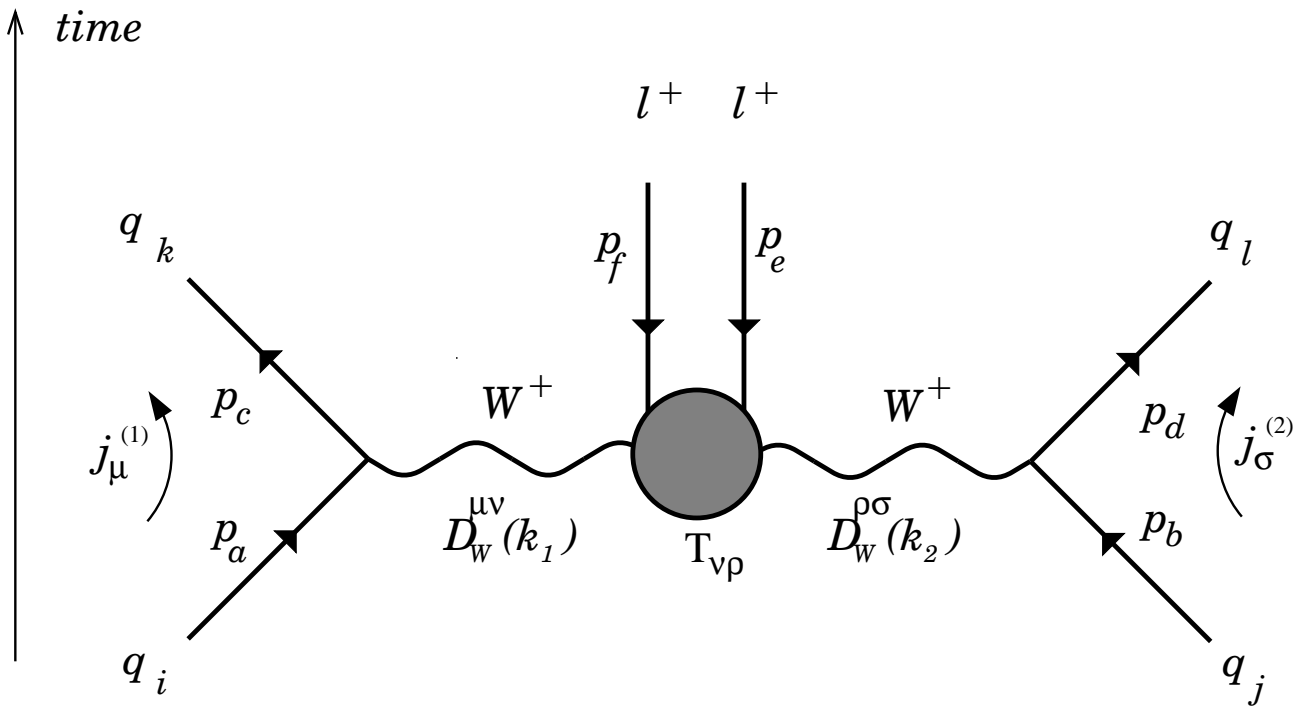


Fig. 2
 O. Panella, C. Carimalo and Y. N. Srivastava
 Physical Review D

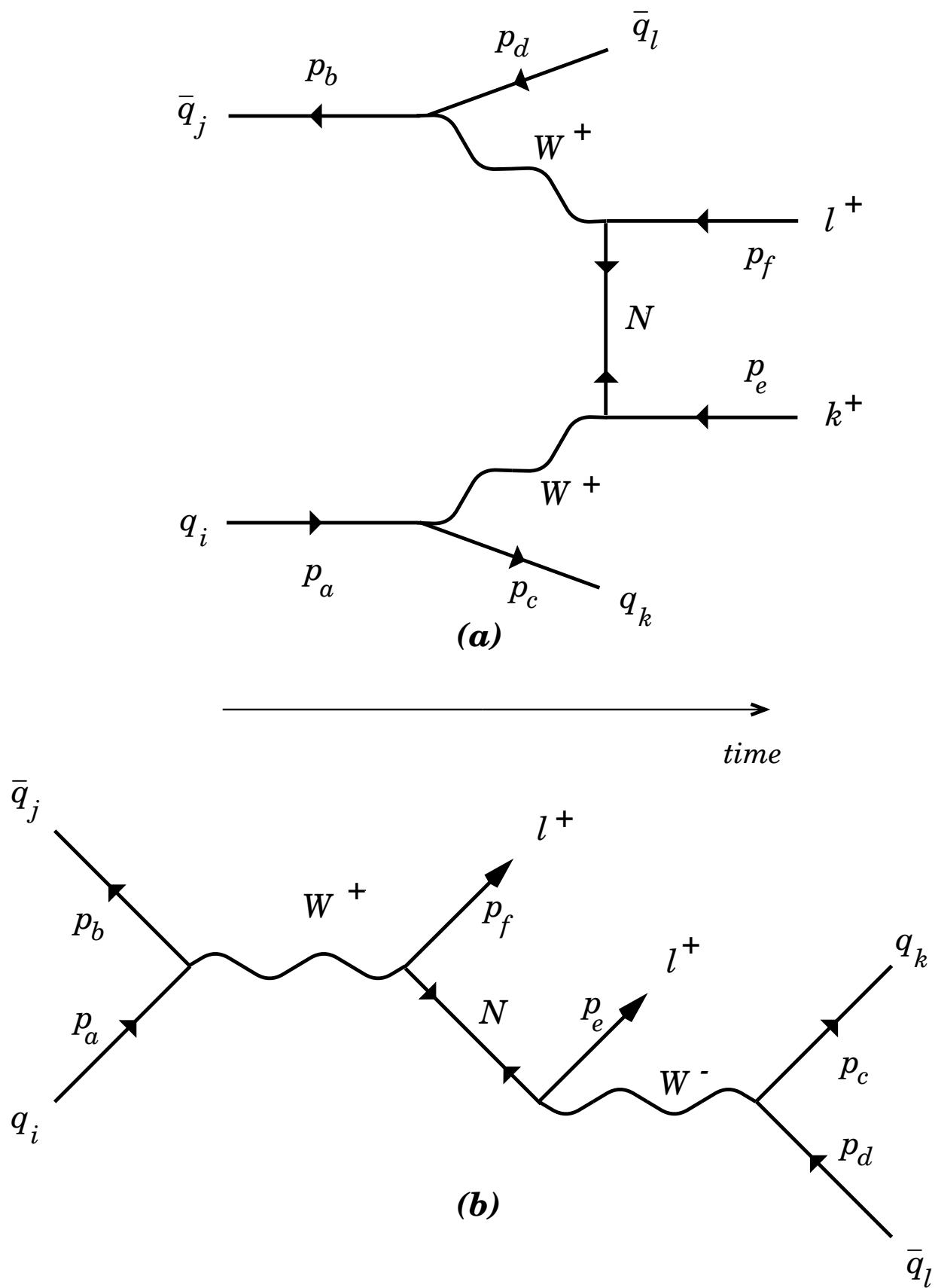
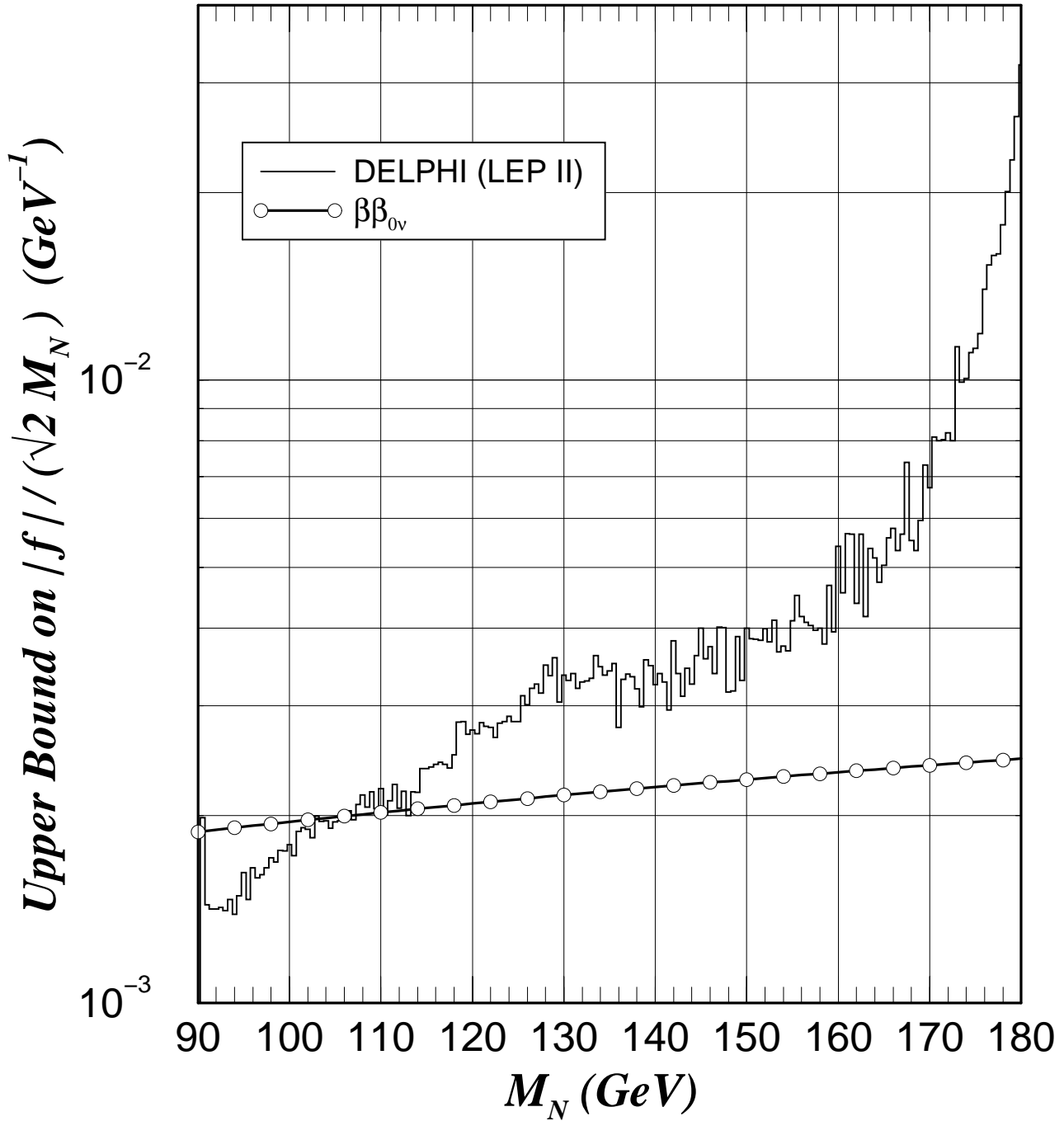


Fig. 3
O. Panella, C. Carimalo and Y. N. Srivastava
Phys. Rev. D.

$$\Lambda_C = M_N$$



Case (a) : $\Lambda_C = 1 \text{ TeV}$; $|f| = 1$

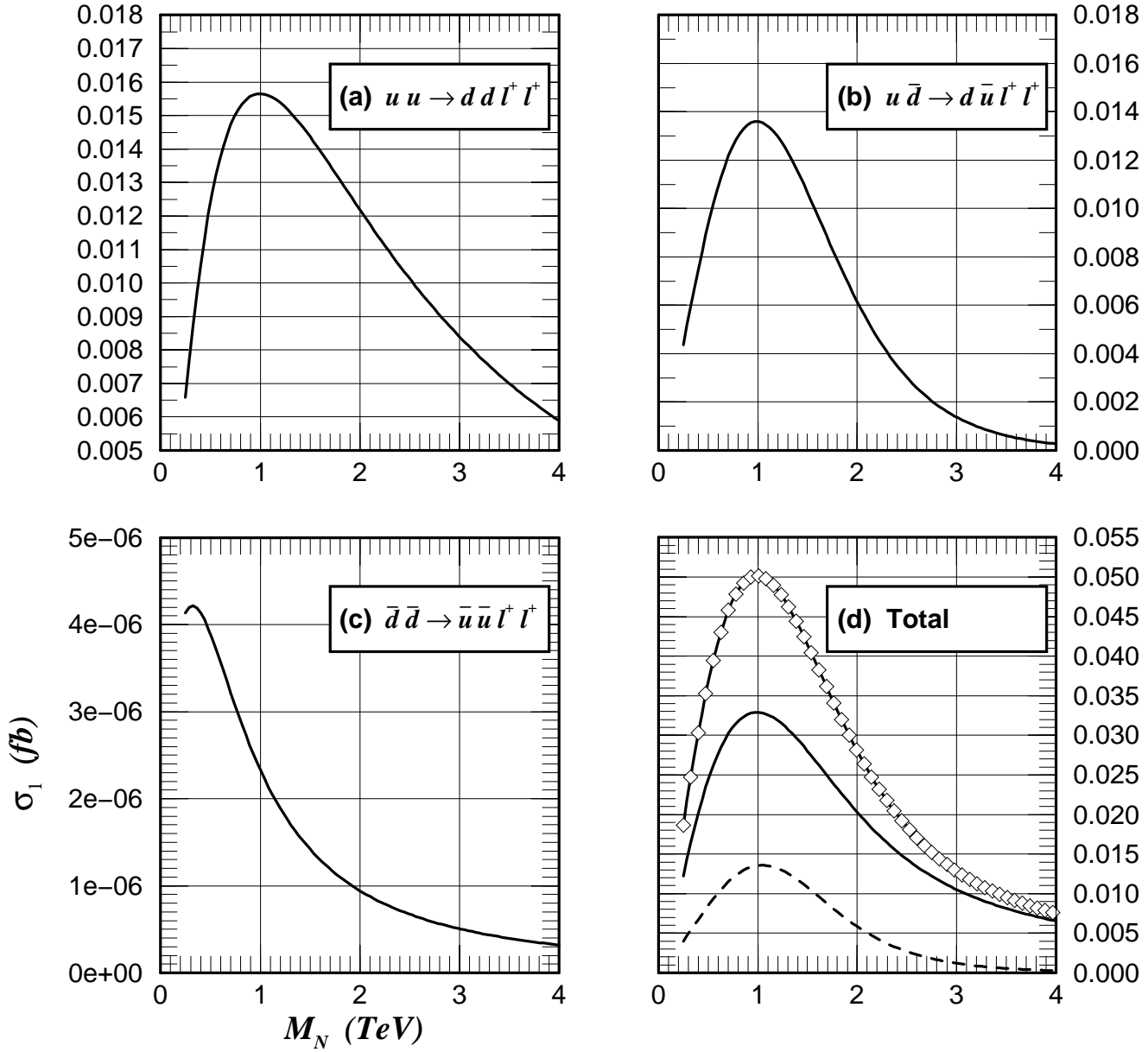
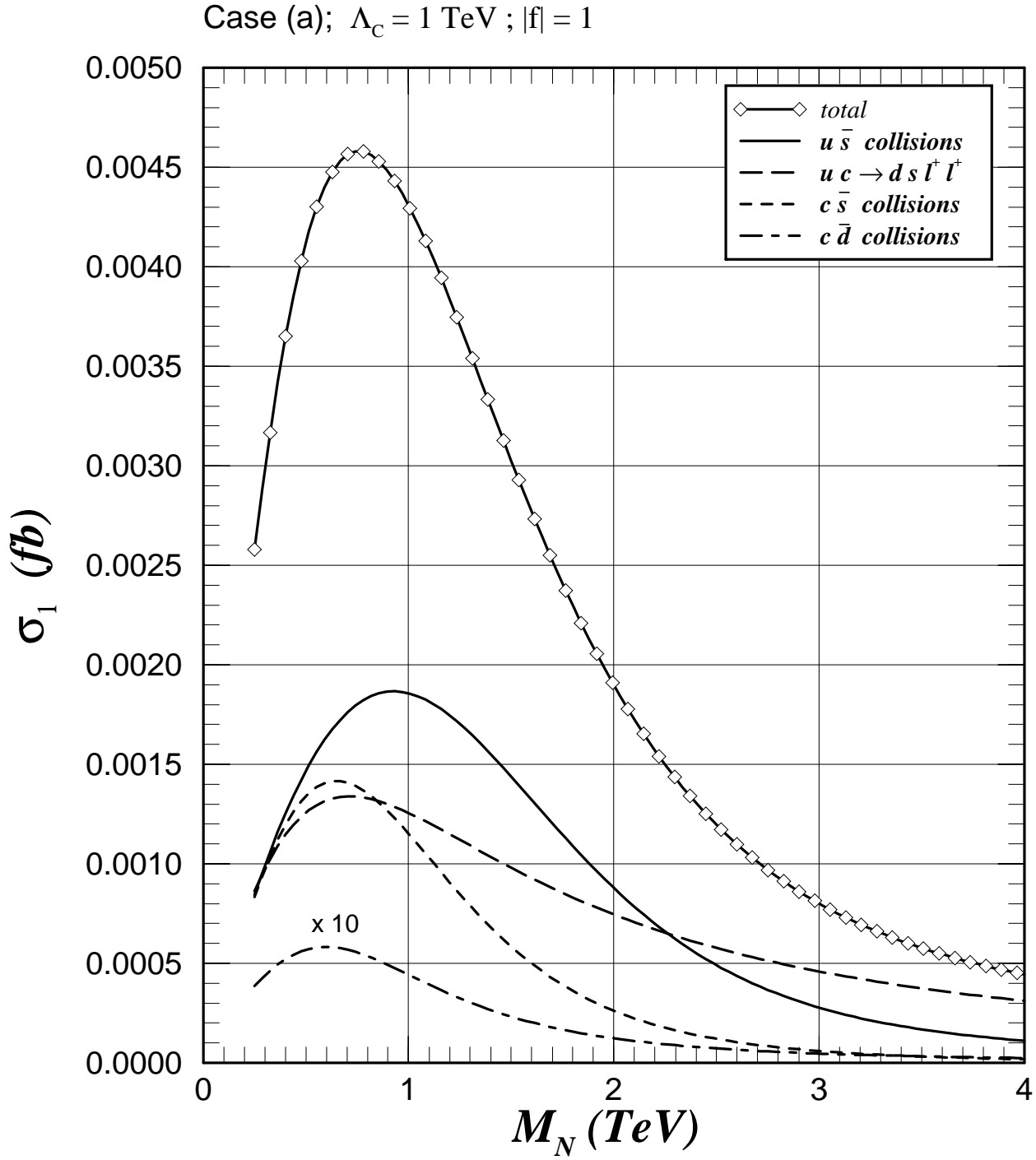
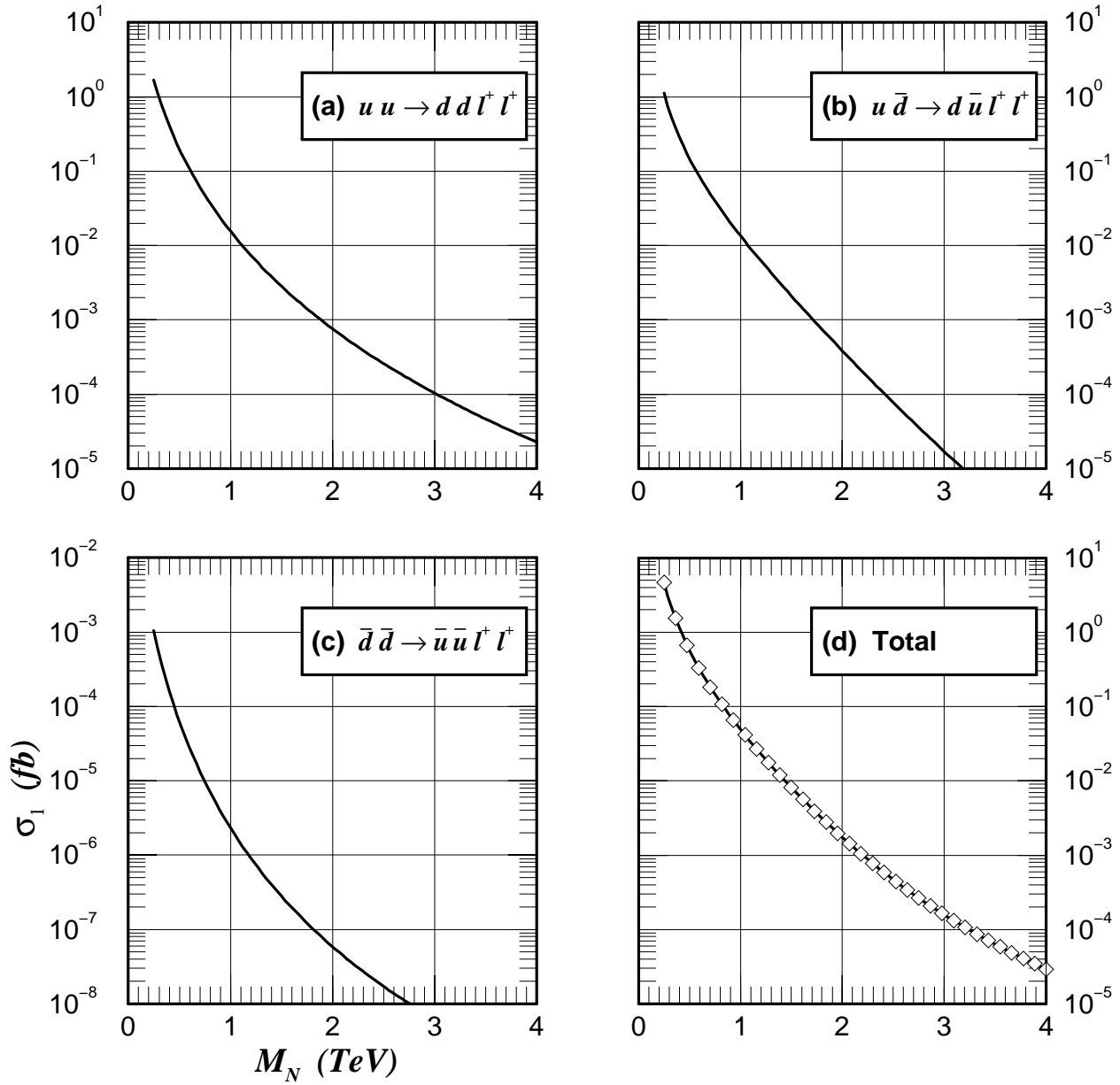


Fig. 5
O. Panella, C. Carimalo and Y. N. Srivastava
Phys. Rev. D.



Case (b) : $\Lambda_C = M_N$; $|f| = 1$



Case (a); $\Lambda_c = 1 \text{ TeV}$

